Journal of the Ceramic Society of Japan 115 [10] 672-677 (2007)

Paper

Solid Electrochemical Micromachining Using a Tungsten Microelectrode Coated with a Polymer Electrolyte

Kai KAMADA,* Masaaki TOKUTOMI, Miki INADA, Naoya ENOMOTO and Junichi HOJO

Department of Applied Chemistry, Faculty of Engineering, Kyushu University, 744, Motooka, Nishi-ku, Fukuoka 819-0395

Electrochemical micromachining of a metal plate was performed using a solid polymer electrolyte. The fundamental electrolysis system was composed of a metal plate (anode)|polymer electrolyte|tungsten needle (cathode), where the contact diameter of the metal|polymer interface was extremely small (a few μm). The metal substrate was electrochemically oxidized and then M^{n+} ions migrated to the polymer electrolyte. As a result of the continuous application of a dc voltage to the cell, finer-resolution micromachining (~10 μm) was achieved under room-temperature operation as compared with our previous results obtained using a Na-β''-Al_2O_3 solid electrolyte. Furthermore, the present technique was applicable to many different kinds of metal substrates. [Received July 3, 2007; Accepted August 24, 2007]

Key-words : *Electrochemical micromachining, Solid polymer electrolyte, Anodic dissolution, Anodic oxidation, Microelectrode*

1. Introduction

Micromachining of solid surfaces is employed for the fabrication of various microsystems, such as microsensors, microreactors, and microelectrode arrays.[1)-3)] It is believed that a more effective and finer-resolution machining technique will be required for dense integration of micro-parts in state-of-the-art microsystems. Micromachining of solid surfaces is generally carried out by position-selective etching of atoms using mechanical, physical and chemical techniques. The chemical technique involves immersion of the workpiece, partly covered with a surface masking layer, in an etching solution, upon which the surface exposed to the solution is selectively dissolved. According to the type of substrate, a patterned layer is preferentially etched by the solution. For instance, the partly pre-formed SiO_2 layer on a Si substrate dissolves in an aqueous HF solution. The fact that no surface distortion or stress is induced in the machined workpiece in the wet chemical process is regarded as a distinct advantage over mechanical or physical (sputtering, laser ablation, etc.) techniques.

As an extension of chemical etching, electrochemical micromachining has been studied widely for conductive substrates such as metals and semiconductors.[4)-6)] In this technique, dissolution of the masked workpiece (electrode) is accelerated by applying an electrical bias to the electrolyte solution. As compared with conventional chemical etching, the electrochemical technique enables a more rapid and well-controlled dissolution rate, and requires no aggressive electrolytes such as an acid. Since electrochemical micromachining employs an electrolyte solution, masking is mandatory for position-selective etching and the process entails multi steps. It is difficult to control the aspect ratio and size of a groove after micromachining because side etching occurs as a result of penetration of liquid under the mask. In order to circumvent these problems, the solid electrochemical method has been proposed,[7),8)] which uses solid ion conductors as an electrolyte, rather than solutions. That is, electrochemical micromachining replaces the liquid electrolyte by a solid electrolyte. Our group has reported that the related solid state technique involves an anodic electrochemical reaction at the microcontact between the metal substrate and ion conductor.[9),10)] The metal substrate is locally incorporated into the ion conductor in the form of metal ions via the microcontact under a dc bias. Micromachining can be achieved as a result of consumption of the metal only at the microcontact. The proposed technique has many advantages over other conventional electrochemical micromachining techniques: (1) no liquid electrolytes, which are difficult to handle, are required, and (2) direct structuring can be achieved without any pretreatments such as masking or coating. Of course, the advantages of the conventional technique, including simplicity of the apparatus and tunability of etching rate and/or size through optimization of electrochemical parameters, are valid in the case of solid systems as well. In our previous reports,[9),10)] a pyramidal Na-β''-Al_2O_3 sintered polycrystal was cut, polished, and used as ion conductor with a sharp apex. However, the reproducible fabrication of β''-Al_2O_3 having a sharp apex is difficult because Na-β''-Al_2O_3 is a hard ceramic material. Thus, the resolution of solid electrochemical micromachining was poor (10^1-10^2 μm). As Na-β''-Al_2O_3 attains high ion conductivity only at high temperature (~873 K), micromachining had to be performed at this temperature range.

In this study, solid electrochemical micromachining was performed using an ion conducting polymer (coated tungsten needle microelectrode) in place of a Na-β''-Al_2O_3 pyramid. As is well known, Nafion has high proton conductivity at room temperature and no anisotropic conduction. Moreover, a variety of metal ions can travel in Nafion in place of protons.[11)] This allows solid electrochemical micromachining of various metals under mild conditions (room temperature). **Figure 1** shows the schematic systems of solid electrochemical micromachining reported in the previous papers[7),8)] (a) and the present study (b). Bard and coworkers[7),8)] have reported selective etching of metal plates (Cu, Ag, Au) coated with a polymer electrolyte film (Fig. 1(a)). However, the etching size would depend on the potential distribution generated in the film. The etching resolution seems lower (10^2 nm) than the point contact between tip and polymer electrolyte film (a few nm^2), and manipulation of the aspect ratio is difficult. In contrast, the present study employs a tungsten (W) microelectrode coated with a polymer electrolyte layer, as depicted in Fig. 1(b). The shape of the apex of an ion conductor can be directly transferred to the metal surface because the solid electrochemical reaction proceeds only at the solid-solid microcontact of the polymer and target metal plate. In other words, the aspect ratio of the machined surface may be easily

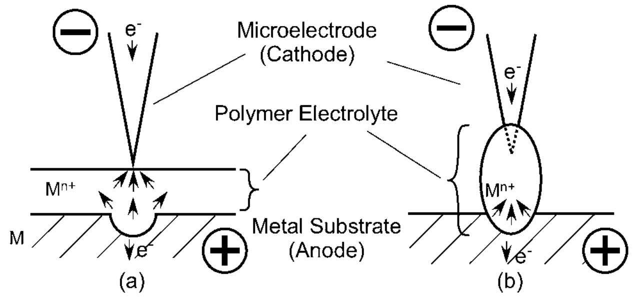

Fig. 1. Schematic system of solid electrochemical micromachining using polymer electrolyte proposed by (a) other group[7] and (b) the present study.

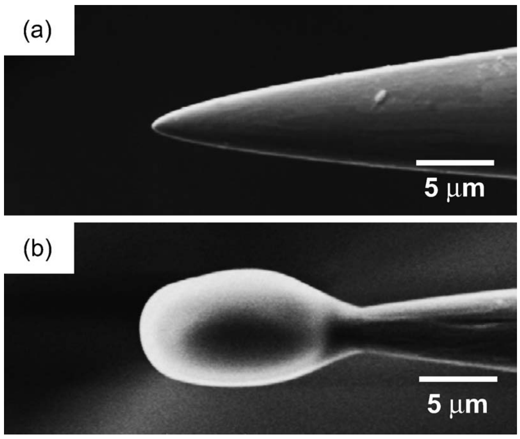

Fig. 2. SEM images of W microelectrode before (a) and after Nafion coating (b).

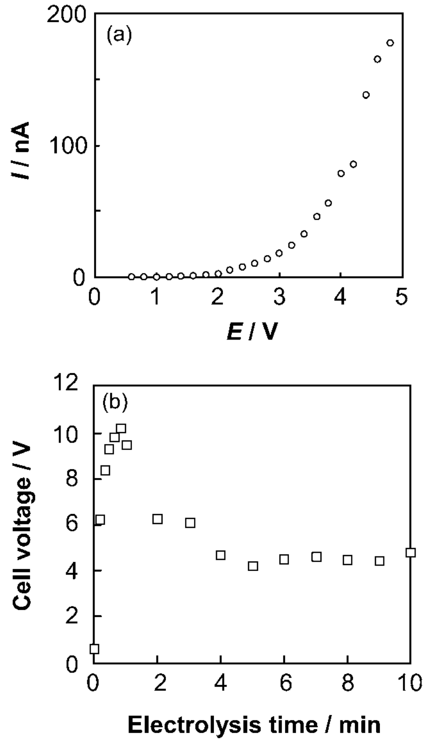

Fig. 3. (a) Polarization curve of (anode) Ag|Nafion|W needle (cathode) (scan rate: 0.2 V/s). (b) Typical change of cell voltage during constant current electrolysis of Ag plate at 1 nA.

designed by the apex configuration of the polymer layer. In the present study, the feasibility and current efficiency of solid electrochemical micromachining of various metals was studied by using various metals as targets. It has been demonstrated that many different kinds of metal substrates can be machined and that submicron resolution can be achieved at room temperature.

2. Experimental procedure

The experimental model is schematized in Fig. 1(b). A Nafion-coated W (Nafion-W) microelectrode was prepared by electrophoretic deposition of Nafion on the apex of a W needle (ca. 1 μm in radius of curvature) in 8 mass% sol solution of Nafion, which was prepared by diluting of 20 mass% solution (DuPont DE2020, Total acid capacity: 0.95–1.03 meq/g) with ethanol. A positive bias was applied to the W needle because Nafion has a negative surface charge according to zeta potential measurements. **Figure 2** shows SEM images of the W microelectrode before (a) and after (b) Nafion coating. Various metal plates (Ag, Cu, Zn, Mg, Fe, Al, and Ti; thickness: 0.1 mm) were used as target of solid electrochemical micromachining. The Nafion-W microelectrode, which was attached to a three-dimensional manipulator, was contacted with a horizontally placed metal plate. The typical metal|Nafion contact diameter was a few μm. This value varied slightly with the apex configuration of the Nafion layer and contact pressure. Solid electrochemical micromachining was performed by applying a constant current or voltage at room temperature and ambient humidity (297–300 K, relative humidity: 25–55%). The slight shift in temperature and humidity did not affect the experimental results. After micromachining, the metal surface was observed by SEM, AFM, and laser microscopy, and the elemental distribution in the Nafion layer was measured by energy dispersive spectroscopy (EDS).

3. Results and discussion

3.1 Ion migration mechanism during solid electrochemical micromachining

Figure 1(b) schematized the mechanism of ion migration observed during solid electrochemical micromachining using a Nafion-W microelectrode. As is well known, Nafion consists of a hydrophobic fluorocarbon chain matrix and hydrophilic proton conduction channels containing $-SO_3H$ groups and H_2O molecules. Protons can migrate via the conduction channel by the Grotthuss and/or vehicle mechanism. When a dc electric field is applied to the cell, the local region of the metal anode at the microcontact is electrochemically oxidized to M^{n+}, which, in turn, is injected into the Nafion via the solid–solid interface. Under a continuous applied electric field, the metal anode is gradually consumed as M^{n+}. Given the small contact size of the metal|Nafion interface (on the order of a few μm), position-selective dissolution occurs at the microcontact, and thus solid electrochemical micromachining is accomplished. At the cathodic interface of Nafion, protons or M^{n+} ions are reduced to H_2 or M, respectively.

3.2 Solid electrochemical micromachining of a silver plate

Solid electrochemical micromachining of a Ag plate was carried out under various conditions. **Figure 3**(a) shows the polarization curve of Ag anode|Nafion|W needle cathode (0.2 V/s). The current was extremely small at low voltage and

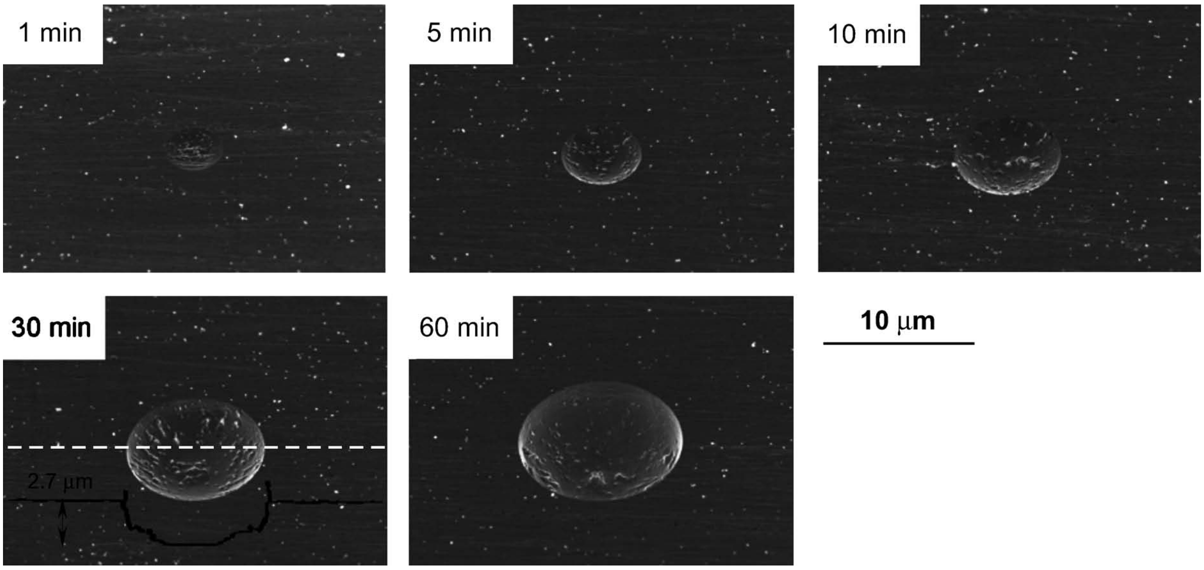

Fig. 4. SEM images of Ag surface after micromachining at 1 nA for various times. Surface profile along the dashed line estimated by a laser microscopy is also shown in "30 min."

increased rapidly above ca. 3 V. Application of a constant electric field of 1 and 3 V for 1 min induced no impressions on the Ag surface. Given the low overvoltage of tungsten cathode for H_2 generation, the actual electric field on the Ag|Nafion interface may be negligible due to the IR drop at the Nafion layer.[7] In contrast, a depression formed at the microcontact as a result of an anodic electrochemical reaction after applying 5 V for 1 min. These results were consistent with the polarization behavior shown in Fig. 3(a). On the other hand, application of a large constant current (~1 μA) caused the Nafion layer to explode through generation of gaseous H_2 at the cathodic interface (Nafion|W). In this case, the current density at the Ag|Nafion interface estimated from circular contact (diameter: 5 μm) was ca. 5 Acm^{-2}. It was considered that such a high current density may cause the rise in temperature at the microcontact and the decomposition of electrolyte. Consequently, a maximum of a few tens of nA was suitable for constant current electrolysis. In following sections, all experiments were performed under galvanostatic conditions in order to determine the current efficiency easily.

Figure 3(b) shows the time evolution of cell voltage during Ag micromachining under 1 nA. The cell voltage rapidly increased to 10 V in the initial stage (<1 min), and then decreased and remained almost constant at about 4 V after 2 min. A similar trend was observed for the Ag|Na–β''–Al_2O_3 microcontact.[10] The initial voltage rise may be due to the inhomogeneous solid–solid contact. Previous papers[12),13)] reporting the current-time behavior at the solid–solid interface of Ag|Ag+ conductors have suggested that the reduction of the actual contact area by electrodifussion and production of atomic scale lattice defects on the Ag surface increases the overvoltage under galvanostatic conditions. This effect becomes much stronger at higher current densities. At longer electrolysis time (>1 min), the increase in apparent contact area with time resulting from embedding the Nafion in Ag (i.e., the decrease in current density) would reduce the overvoltage. **Figure 4** shows SEM images of Ag surfaces after solid electrochemical micromachining at 1 nA for various durations. All SEM samples were held at a 40° incline with respect to the perpendicular electron beam axis. The center of the

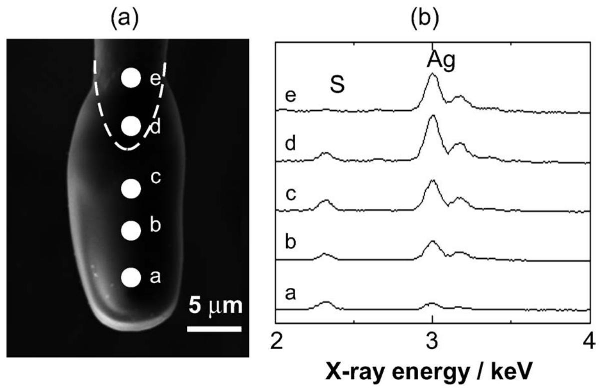

Fig. 5. (a) SEM image of the Nafion layer after machining at 1 nA for 30 min. (b) EDS spectra for the points shown in (a).

micrographs corresponds to the Ag|Nafion microcontact. The mechanical stress caused by the Nafion-W microelectrode could be ignored because no change occurred in the absence of the electric field. Figure 4 indicates that the Ag plate was locally etched according to the apex form of the Nafion layer, i.e., a quasi-hemisphere less than 10 μm in diameter. The tiny projections seen on the surface of the depression may be due to the inhomogeneous distribution of hydrophilic channels in the hydrophobic matrix. The fact that the sharp edge of the depressions is clearly visible indicates that the solid electrochemical reaction occurred only at the Ag|Nafion microcontact. Thus, no side etching occurred during micromachining, which is one of the main advantages of the present technique. Naturally, the diameter of the quasi-hemisphere increased with electrolysis time.

Figure 5(a) shows an SEM image of the Nafion-W microelectrode after solid electrochemical micromachining (1 nA, 30 min), where the dashed line indicates the position of the W apex implanted in the Nafion layer. The EDS spectra at points a through e in Fig. 5(a) are presented in Fig. 5(b). Ag was detected in the spectra in addition to the S from Nafion. This indicates that the electrochemical diffusion of Ag^+ from the

Ag plate into the Nafion was induced by the dc bias. Thus, the ion migration mechanism proposed above was indeed at play during electrolysis. The characteristic X-ray intensity of Ag, which is indicative of the Ag concentration, increased with increasing distance from the microcontact $(a>b>c>d>e)$. The Ag^+ that diffused through the Nafion layer was reduced and accumulated at the cathodic Nafion|W interface.[14] A short circuit between the Ag plate and W needle was constructed by Ag deposition inside the Nafion at longer electrolysis times or using a thinner Nafion layer. In summary, it was demonstrated that a Nafion-coated W microelectrode enables solid electrochemical micromachining under relatively mild conditions (room temperature) and with finer precision (<10 μm) than is achievable using Na-β''-Al_2O_3. In the previous method described in Fig. 1(a), metallic deposits produced at the polymer|tip cathode interface increased the etching dimension. In the present study, no expansion of machining size was observed using the Nafion-W microelectrode, and the apex configuration of the Nafion layer was directly transferred to the surface of the workpiece. That is, the machining accuracy and aspect ratio depended only on the apex dimensions of the Nafion layer.

3.3 Evaluation of current efficiency of Ag micromachining

The machining size appears to be tunable by adjusting the applied electricity, which is related to the electrolysis time under galvanostatic conditions. The electrolysis time evolution of the machining size was investigated for a Ag plate at a constant current of 1 nA. **Figure 6**(a) shows the time dependence of the machining volume estimated on the basis of a surface profile obtained by laser microscopy. The depressions were assumed to be a part of a sphere, and then their volumes were calculated from the diameter and depth. The current efficiencies estimated from the machining volume, applied electricity, and density of silver using Faraday's law are also plotted in Fig. 6(a). The depression volume increased continuously as time progressed. Thus, machining size can be easily controlled to within about 10^0–10^2 μm^3 by varying electrochemical parameters such as electrolysis time and/or current. The current efficiencies also increased with electrolysis time, and reached 68% at 60 min. The leakage current is expected to be consumed by proton conduction in the Nafion layer. As described in Fig. 6(b), electrolysis of H_2O in air is likely to induce the production of H^+ via the three phase boundary during the initial stage. At longer electrolysis times, the Nafion layer became embedded in the Ag plate, and the Ag|Nafion contact area increased. Consequently, dissolution of the Ag plate was favored over moisture electrolysis, and the current efficiency was enhanced. The maximum current efficiency in the present study was much higher than that obtained using Na-β''-Al_2O_3 (about 40%). That is, the Nafion-W microelectrode enabled much more efficient solid electrochemical micromachining and under mild conditions.

3.4 Solid electrochemical micromachining of Cu, Zn, Mg, and Fe

Nafion is a unique material because numerous types of metal ions can be incorporated into the hydrophilic conduction channels instead of protons. That is, a variety of different kinds of metal substrates can presumably be used as a workpiece. Hence, solid electrochemical micromachining of various metal plates was attempted. In general, metals can be easily oxidized at high temperature in an oxidizing atmosphere, whereby a thick oxide film is formed on surface. In the case of micromachining using Na-β''-Al_2O_3 at high temperature, the presence of the oxide film suppresses the anodic dissolution of metal, and an inert atmosphere is required to prevent surface

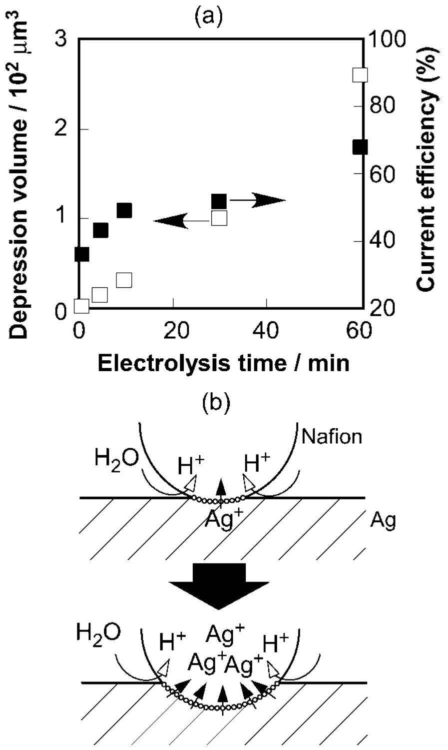

Fig. 6. (a) Electrolysis time dependence of machining volume and current efficiency of Ag micromachining under a constant applied current of 1 nA. (b) Change of dominant carrier in the Nafion layer.

oxidation. Also, metals having a low melting temperature could not be employed as a target of micromachining. Owing to the high ion conductivity of Nafion even at room temperature, various kinds of metals can be used as a target without the restrictions mentioned above. **Figure 7** shows SEM images of the surface of Cu, Zn, and Mg plates after solid electrochemical micromachining. The images suggest that the depressions were produced during electrolysis in similar manner to the Ag plate. EDS analysis revealed the presence of each metallic element in the Nafion layer after electrolysis. Hence, solid electrochemical micromachining of these metals may also be possible. As shown in Fig. 7, the surfaces of the depressions were rougher than those in the case of Ag. It has been reported that the exchange current between the Cu^{2+} dissolving in Nafion and the Cu plate coarsened the surface.[7] The variations in cell voltage observed in the case of Cu, Zn, Mg, and Fe were quite different from that in the case of Ag, and tended to increase with time. According to the EDS spectra, a small amount of oxygen was detected in the metal surfaces. The oxide (hydroxide, hydrated oxide) formed on the surface anodically, accompanied by the anodic dissolution. Table 1 summarizes the results of solid electrochemical micromachining for given constant current values. Cu and Fe were presumed to be dissolved as Cu^{2+} and Fe^{3+}, respectively.[15] The current efficiencies of Cu, Zn, Mg, and Fe were one~two orders magnitude lower than that of Ag. It was reported that the substitution of small amount of metal ions (~30%) for protons does not interrupt the ion conduction in Nafion.[11] Therefore, the surface oxide would act as a barrier to anodic dissolution. This is thought to be the main reason for the low efficiencies. **Table 1** also indicates that applying a larger constant current reduces the efficiency, and thus, a smaller current is more appropriate for effective micro-

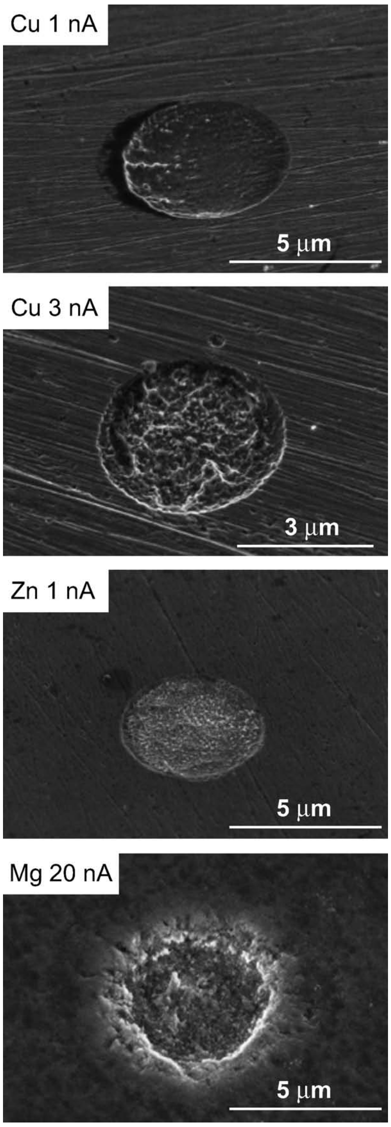

Fig. 7. SEM images of etched metal surfaces under various conditions for 60 min.

Table 1. Machining Volumes and Current Efficiencies of Solid Electrochemical Micromachining (60 min)

Target	I / nA	Machining volume / μm^3	Current efficiency (%)
Ag	1	260	67.7
Cu	1	8.9	6.7
	3	1.8	0.5
Zn	1	3.2	1.8
	3	3.1	0.6
Mg	10	9.0	0.4
	20	9.8	0.2
Fe	5	2.5	0.6
Al	20	—	
Ti	5	—	

machining.

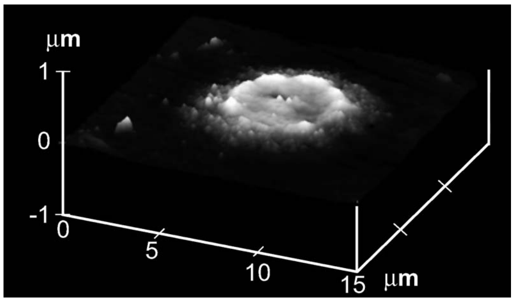

Fig. 8. AFM image of Al plate after applying 20 nA for 60 min.

3.5 Anodic electrolysis of Al and Ti using the Nafion-W microelectrode

In the case of the Al and Ti workpieces, no local anodic dissolution was detected; a passive oxide layer formed on their surface. **Figure 8** is an AFM image taken near the microcontact of the Al surface after electrolysis at 20 nA for 60 min. Clearly, the metal surface around the microcontact has lifted off. SEM observation and EDS analysis of the cross-section of Al and Ti plates revealed that the surface layer consists of a dense oxide film. As shown in Fig. 8, the thicker oxide layer formed along the circumference of the microcontact between Nafion and Al. Thus, oxide growth was promoted at the three phase boundary. It was confirmed that Al^{3+} or TiO^{2+} can be exchanged in the Nafion membrane by immersion in an aqueous $AlCl_3$ or $TiOCl_2$ solution. However, no evidence of anodic dissolution of Al or Ti was found in the present study. In the case of Al and Ti, the metal ions migrating through the oxide film reacted readily with H_2O and induced the growth of a thick passive layer. Although Mg also produces an anodic oxide film in aqueous solution, similarly to Al and Ti, solid electrochemical micromachining was successful, as shown in Fig. 7. It is well known that Mg is not coated with a barrier (dense) oxide film by anodic treatment because the volume ratio of oxide/metal is smaller than unity. The local dissolution of Mg^{2+} may proceed via the defects in the passive oxide layer. The high solubility of Mg^{2+} in neutral to acidic solutions[16] may also be one of the reasons for the local dissolution of Mg observed when using the Nafion-W microelectrode. Thus, metals that form a dense and chemically stable surface oxide are difficult to micromachine by the present technique. Nevertheless, it may be possible to pattern the oxide layer using the Nafion-W microelectrode.

3.6 Fabrication of etching pattern by scanning Nafion-W microelectrode

Solid electrochemical micromachining occurs only at the solid–solid interface between Nafion and the metal substrate. Thus, micromachining could conceivably enable the fabrication of patterned metal substrates if the Nafion-W microelectrode were to be moved along the metal surface during electrolysis. To groove the Ag plate on a submicron scale, a Nafion-W microelectrode equipped with a three-dimensional manipulator was scanned along the Ag surface under an applied electric field; a W microelectrode coated with a thin Nafion layer ($<1\,\mu$m) was used to attain fine resolution. **Figure 9** is an AFM image of an Ag surface obtained by scanning the Nafion-W microelectrode (50 nm/s) at 1 nA. As expected, a single track was produced along the pathway of the microelectrode. Thus, scanning of the Nafion-W microelectrode yielded a micropattern of tracks on a submicron scale (width: 0.4 μm, depth: 0.1 μm). Furthermore, it was

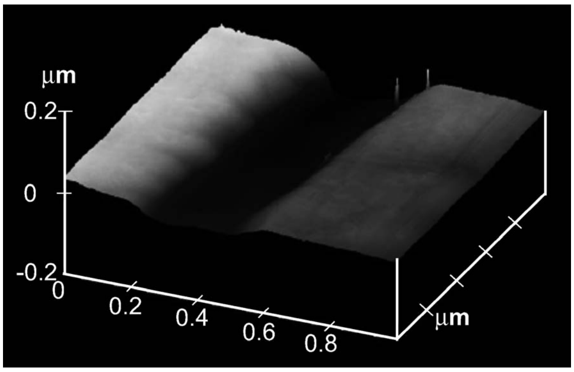

Fig. 9. AFM image of Ag surface (1 nA) after scanning with a Nafion-W microelectrode (10 μm/s).

confirmed that increasing the constant current broadened the line and that the width at any given current was inversely proportional to the scan rate. That is, the track size depended on the current applied per unit area per unit time. As the fundamental micromachining mechanism is the same as in the case of the fixed microelectrode, a variety of metal substrates can be patterned by manipulating the ion conductor. Since the Nafion-W microelectrode is attached to the manipulator, a variety of patterns, including not only simple patterns (line or dot), but also more complex structures, can be fabricated to meet specific design criteria.

4. Conclusions

The present study demonstrated that the use of a Nafion-coated tungsten microelectrode enables solid electrochemical micromachining of metal substrates with high resolution at ambient condition. The metal substrates were dissolved locally and anodically at the microcontact with the ion-conducting Nafion. The accuracy of micromachining was improved as compared with our previous reports using Na-β''-Al_2O_3, and room-temperature operation was achieved. The present technique was applied to various metal substrates (Ag, Cu, Zn, etc.). By coating a W microelectrode with Nafion, the apex shape of a Nafion layer could be transferred directly to the metal surface without any detectable side etching or expansion of machining dimensions. The formation of a surface oxide caused a current loss, which indicated that a lower applied current or electric field is more appropriate for efficient micromachining. Electrochemical etching on a submicron scale has already been accomplished by liquid and solid systems. Thus, control of the apex shape of the Nafion-W microelectrode and optimization of electrochemical parameters will improve the machining accuracy and yield the desired aspect ratio. The electrochemical technique enables micromachining without any mechanical stress or distortion to the substrate. Thus, the proposed technique may be effective in local thinning of TEM samples. In the near future, the present technique is expected to grow as one of many new applications of solid polymer electrolytes, such as actuators[17),18)] and sensors.[19),20)]

Acknowledgements The present work was partly supported by the Asahi Glass Foundation, Japan and Grant-in-Aid for Young Scientists (A) No. 17685022, and on Priority Area "Nanoionics (439)" No. 17041014 from the Ministry of Education, Culture, Sports, Science, and Technology, Japan.

References

1) J. W. Schultze and V. Tsakova, *Electrochim. Acta*, **44**, 3605–3627 (1999).
2) D. Xu, L. Wang, G. Ding, Y. Zhou, A. Yu and B. Cai, *Sens. Actuators A*, **93**, 87–92 (2001).
3) Y. S. S. Wan, J. L. H. Chau, A. Gavriilidis and K. L. Yeoung, *Microporous Mesoporous Mater.*, **42**, 157–175 (2001).
4) W.-H. Chang, *Sens. Actuators A*, **112**, 36–43 (2004).
5) P.-F. Chauvy, P. Hoffman and D. Landolt, *Appl. Surf. Sci.*, **211**, 113–127 (2003).
6) P.-F. Chauvy, P. Hoffman and D. Landolt, *Electrochem. Solid-State Lett.*, **4**, C31–C34 (2001).
7) O. E. Husser, D. H. Craston and A. J. Bard, *J. Vac. Sci. Technol. B*, **6**, 1873–1876 (1988).
8) O. E. Husser, D. H. Craston and A. J. Bard, *J. Electrochem. Soc.*, **136**, 3222–3229 (1989).
9) K. Kamada, K. Izawa, Y. Tsutsumi, S. Yamashita, N. Enomoto, J. Hojo and Y. Matsumoto, *Chem. Mater.*, **17**, 1930–1932 (2005); *Correction*, **18**, 1713 (2006).
10) K. Kamada, M. Tokutomi, N. Enomoto and J. Hojo, *Electrochim. Acta*, **52**, 3739–3745 (2007).
11) N. Yoshida, T. Ishisaki, A. Watakabe and M. Yoshitake, *Electrochim. Acta*, **43**, 3749–3754 (1998).
12) J. Janek and S. Majoni, *Ber. Bunsenges. Phys. Chem.*, **99**, 14–20 (1995).
13) S. Majoni and J. Janek, *Solid State Ionics*, **85**, 247–250 (1996).
14) J. Chou, E. W. McFarland and H. Metiu, *J. Phys. Chem. B*, **109**, 3252–3256 (2005).
15) M. I. Ahmed, H. T. Chang, J. R. Selman and T. M. Holsen, *J. Membr. Sci.*, **197**, 63–74 (2002).
16) M. Pourbaix, "Atlas of Electrochemical Equilibria in Aqueous Solutions," National Association of Corrosion Engineers, Texas (1974) pp. 139–145.
17) S. Nemat-Nasser and J. Y. Li, *J. Appl. Phys.*, **87**, 3321–3331 (2000).
18) J. W. Paquette, K. J. Kim and D. Kim, *Sens. Actuators A*, **118**, 135–143 (2005).
19) S. Legeai and O. Vittori, *Anal. Chim. Acta*, **560**, 184–190 (2006).
20) L.-X. Sun and T. Okada, *Anal. Chim. Acta*, **421**, 83–92 (2000).